INTERNATIONAL JOURNAL FOR NUMERICAL METHODS IN ENGINEERING
Int. J. Numer. Meth. Engng 2003; **57**:1039–1052 (DOI: 10.1002/nme.708)

A shell problem 'highly sensitive' to thickness changes[‡]

Klaus-Jürgen Bathe[1,*,†], Dominique Chapelle[2] and Phill-Seung Lee[1]

[1]*Department of Mechanical Engineering, Massachusetts Institute of Technology, Cambridge, MA 02139, U.S.A.*
[2]*INRIA-Rocquencourt, B.P. 105, 78153 Le Chesnay cedex, France*

SUMMARY

In general, shell structural problems can be identified to fall into one of the categories of membrane-dominated, bending-dominated and mixed shell problems. The asymptotic behaviour with a well-defined load-scaling factor shows distinctly into which category a given shell problem falls. The objective of this paper is to present a shell problem and its solution for which there is no convergence to a well-defined load-scaling factor as the thickness of the shell decreases. Such shells are unduly sensitive in their behaviour because the ratio of membrane to bending energy stored changes significantly and indeed can fluctuate with changes in shell thickness. We briefly review the different asymptotic behaviours that shell problems can display, and then present the specific problem considered and its numerical solution using finite element analysis. Copyright © 2003 John Wiley & Sons, Ltd.

KEY WORDS: shells; asymptotic analysis; finite element solution

1. INTRODUCTION

The classification of shell problems into membrane-dominated, bending-dominated and mixed problems has been used for a long time, see for example References [1, 2]. However, only relatively recently, this categorization has been made more precise by considering the asymptotic behaviours of shells. For a detailed discussion of the asymptotic behaviours of shell structures and some solution results, we refer to References [3–10], but for completeness of this presentation we give a short summary.

Let us consider a shell mathematical model governed by equations that in variational form result in the problem statement

$$\text{Find } u^\varepsilon \in V \text{ such that}$$
$$\varepsilon^3 A_\mathrm{b}(u^\varepsilon, v) + \varepsilon A_\mathrm{m}(u^\varepsilon, v) = F^\varepsilon(v), \quad \forall v \in V \tag{1}$$

*Correspondence to: Klaus-Jürgen Bathe, Department of Mechanical Engineering, Massachusetts Institute of Technology, Cambridge, MA 02139, U.S.A.
†E-mail: kjb@mit.edu

‡Because of the high sensitivity of the shell, and the difficulties in the mathematical and numerical analyses, we frequently refer colloquially to the problem as a 'monster shell problem'.

Received 24 April 2002
Revised 29 July 2002
Accepted 30 August 2002

where ε is the shell thickness parameter t/L (t is the thickness and L is a global characteristic dimension of the shell structure), the bilinear form A_b represents the scaled bending energy, the bilinear form A_m represents the scaled membrane energy and, if shear deformations are included, also the scaled shear energy, u^ε is the unknown solution (displacement field), v is the test function, V is the appropriate Sobolev space, and F^ε denotes the external loading. We emphasize that the bilinear forms A_b and A_m are independent of the thickness parameter ε. Since the shear energy is zero or small, we refer to the term in Equation (1) corresponding to A_m, in brief, as the membrane energy term.

To study the behaviour of the shell as ε approaches zero, we introduce the scaled loading in the form

$$F^\varepsilon(v) = \varepsilon^\rho G(v) \tag{2}$$

where G is an element of V' independent of ε, and ρ is a real number for which the scaled external work $G(u^\varepsilon)$ converges to a finite and non-zero limit as ε tends to zero. It can be proven that, when such a well-defined scaling exists, we have $1 \leqslant \rho \leqslant 3$, see for example, Reference [8].

The following space plays a crucial role in determining what asymptotic behaviour will be observed as ε approaches zero [10]

$$V_0 = \{v \in V \mid A_m(v, v) = 0\} \tag{3}$$

This space is the subspace of 'pure bending displacements' and corresponds to all displacement patterns in V with zero membrane and shear energies. When the content of this subspace is only the zero displacement field ($V_0 = \{0\}$), we say that 'pure bending is inhibited' (or, in short, we have an 'inhibited shell'). On the other hand, when the shell admits non-zero pure-bending displacements, we say that 'pure bending is non-inhibited' (we have a 'non-inhibited shell'). The asymptotic behaviour of shells is highly dependent on whether or not pure bending is inhibited.

The 'pure bending is non-inhibited' situation (that is, the case $V_0 \neq \{0\}$) frequently results in the bending-dominated state. Then the appropriate value to use for the load-scaling factor ρ is 3, the membrane energy term of Equation (1) asymptotically vanishes and the general form of the limit problem is

$$\begin{aligned} &\text{Find } u^0 \in V_0 \text{ such that} \\ &A_b(u^0, v) = G(v), \quad \forall v \in V_0 \end{aligned} \tag{4}$$

This limit problem holds only when the loading activates the pure-bending displacements. In case the loading does not activate the pure-bending displacements, the theoretical asymptotic behaviour is as for the pure-bending inhibited case, but very unstable [10]. Namely, a small perturbation in the loading that activates the pure-bending displacements will change the asymptotic behaviour to the bending-dominated state.

Considering the 'pure bending is inhibited' situation (that is, the case $V_0 = \{0\}$), we use the load-scaling factor $\rho = 1$ and, provided the problem is well posed, obtain the limit problem of the membrane-dominated case in the space V_m consisting of all displacements of bounded membrane and shear energies only. Therefore, this space is larger than V. The general form

Table I. The classification of shell asymptotic behaviours.

Case	Loading	Category
Non-inhibited shell $V_0 \neq \{0\}$	Loading activates pure-bending displacements $\exists v \in V_0$ such that $G(v) \neq 0$	(i) Bending dominated
	Loading does not activate pure-bending displacements $G(v) = 0$, $\forall v \in V_0$	(ii) Membrane dominated or mixed but unstable
Inhibited shell $V_0 = \{0\}$	Admissible membrane loading $G \in V_m'$	(iii) Membrane dominated
	Non-admissible membrane loading $G \notin V_m'$	(iv) Mixed

of the membrane-dominated limit problem is

$$\text{Find } u^m \in V_m \text{ such that}$$

$$A_m(u^m, v) = G(v), \quad \forall v \in V_m \tag{5}$$

and this problem is well posed provided the loading G is in the dual space of V_m. The condition $G \in V_m'$ is directly equivalent to

$$|G(v)| \leqslant C\sqrt{A_m(v,v)}, \quad \forall v \in V \tag{6}$$

with C a constant. Equation (6) ensures that the applied loading can be resisted by membrane stresses only, and hence the condition $G \in V_m'$ is said to correspond to an 'admissible membrane loading'. If the loading is a non-admissible membrane loading ($G \notin V_m'$), we have an ill-posed membrane problem. The asymptotic state then does not correspond to membrane energy only, and the shell problem is classified as a mixed problem. Note that when V_m is large, its dual space is correspondingly small and the applied loading is more likely to lead to a mixed problem.

Table I summarizes the asymptotic categories of shell behaviours. The important point is that for the shell problems referred to in Table I, for cases (i) and (iii) we have the well-defined values of $\rho = 3$ and 1, respectively, and considering the mixed case, generally, we also have a well-defined load-scaling factor. In each of these cases, the value of ρ then clearly displays the category to which this shell problem belongs, the percentage of bending and membrane energies stored asymptotically in the shell, and hence physically the load carrying capacity of the shell.

Various numerical schemes to calculate the load-scaling factor have been presented by Lee and Bathe [9]. One simple way to proceed is to solve the shell problem with a constant load application and then evaluate for decreasing values of ε,

$$\bar{\rho} = -\frac{\log E(\varepsilon_1) - \log E(\varepsilon_2)}{\log \varepsilon_1 - \log \varepsilon_2} \tag{7}$$

where $E(\varepsilon_1)$ and $E(\varepsilon_2)$ are, respectively, the total strain energies corresponding to ε_1 and ε_2 when a constant loading is applied. Then we have

$$\rho = \lim_{\varepsilon_1, \varepsilon_2 \to 0} \bar{\rho} \tag{8}$$

Lee and Bathe [9] solved, using finite element analysis, for the asymptotic behaviour of three shell problems, one from each category (i), (iii) and (iv). The problems solved were a hyperbolic paraboloid shell problem, the original Scordelis–Lo roof problem and a modified Scordelis–Lo roof problem. These problems showed clear asymptotic states in the numerical studies corresponding to bending-dominated ($\rho = 3$), mixed ($\rho \approx 1.73$)[§] and membrane-dominated ($\rho = 1$) behaviours, respectively.

Based on the experiences published regarding shell analyses, it may appear that all shell problems, in the three categories discussed above, have well-defined values of load-scaling factors. But there is of course no mathematical proof available on which to base this expectation. Indeed, our objective with this paper is to present a problem, and its solution, which does not have a well-defined load-scaling factor for the thickness values considered. These values range from $\varepsilon = 0.01$ to 10^{-6}, with the very small values included in order to identify numerically the asymptotic behaviour (although such small values may, at present, be considered not practical). We selected this problem inspired by the analytical studies on simplified cases presented by Pitkäranta and Sanchez-Palencia [11]. Physically, the shell considered is an unduly sensitive structure in the sense that the spatial distribution of displacement and stress response changes significantly with changes in the shell thickness. And associated with this phenomenon, the ratio of bending energy to total strain energy stored in the shell changes and does not converge to a specific value as the shell thickness decreases.

2. THE SHELL PROBLEM AND ITS SOLUTION

Figure 1 shows the problem considered. The shell geometry corresponds to a half-sphere with the top sliced off. The shell is clamped around its entire lower boundary. The loading corresponds to a smoothly distributed pressure load over a small part of the interior of the shell. We perform a linear elastic analysis, assuming infinitesimally small displacements and elastic isotropic material conditions.

For the finite element solutions, we use the MITC 4-node shell element in ADINA [12]. The element implementation is based on the 'basic shell model' discussed by Chapelle and Bathe [13]. The 'basic shell model' equations have the same asymptotic behaviour as the models considered in Equation (1) when the thickness of the shell decreases, and hence the discussion in Section 1 regarding the asymptotic behaviours applies.

Figure 2 shows the finite element mesh used, which consists of 32 (axial) by 128 (circumferential) shell elements. This is a sufficiently fine mesh to identify and reasonably resolve boundary layers. (For this mesh, the total solution time on a Pentium III PC has only been about 10 sec.) The loading was applied by first calculating the load intensities given by the

[§]An analytical value of ρ can actually be obtained for the original Scordelis–Lo roof shell problem and this value is $\rho = 1.75$ [8].

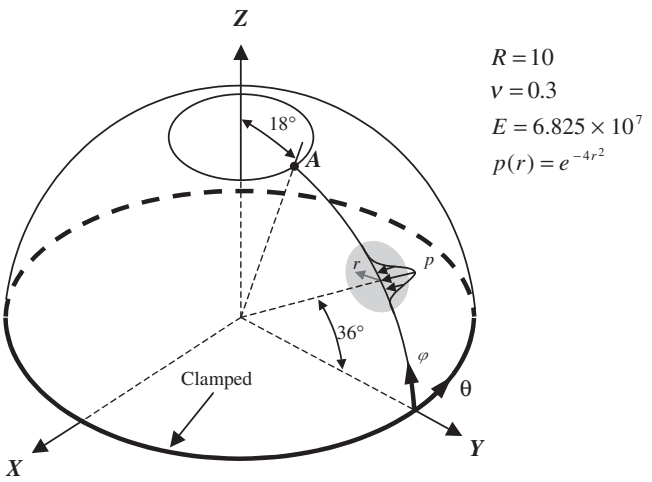

Figure 1. The shell problem, $L = R$.

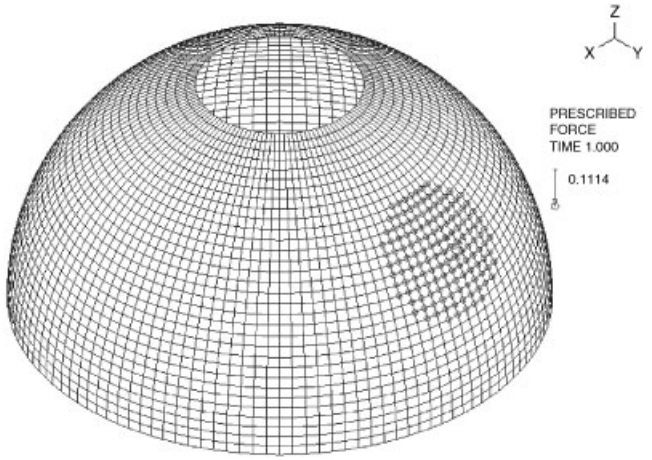

Figure 2. The finite element mesh used (the loaded area is also shown).

pressure distribution at the element nodes. Then the consistent nodal point forces corresponding to the pressure interpolated over the elements were evaluated.

Figure 3 shows the calculated displacements of the shell as we decrease the shell thickness. For plotting, the displacements are normalized in the figure so that the maximum outward total displacement value is equal to 3.0. We note that when the thickness is small (that is, $t/L < 1/100$), the displacements are dominant in the immediate vicinity of the boundary, namely within a boundary layer. This boundary layer has a width of the order $L/\log(1/\varepsilon)$, see Figure 4. In addition, the displacements in the boundary layer oscillate in the circumferential direction, with the number of oscillations given by $\log(1/\varepsilon)$; that is, the number of oscillations

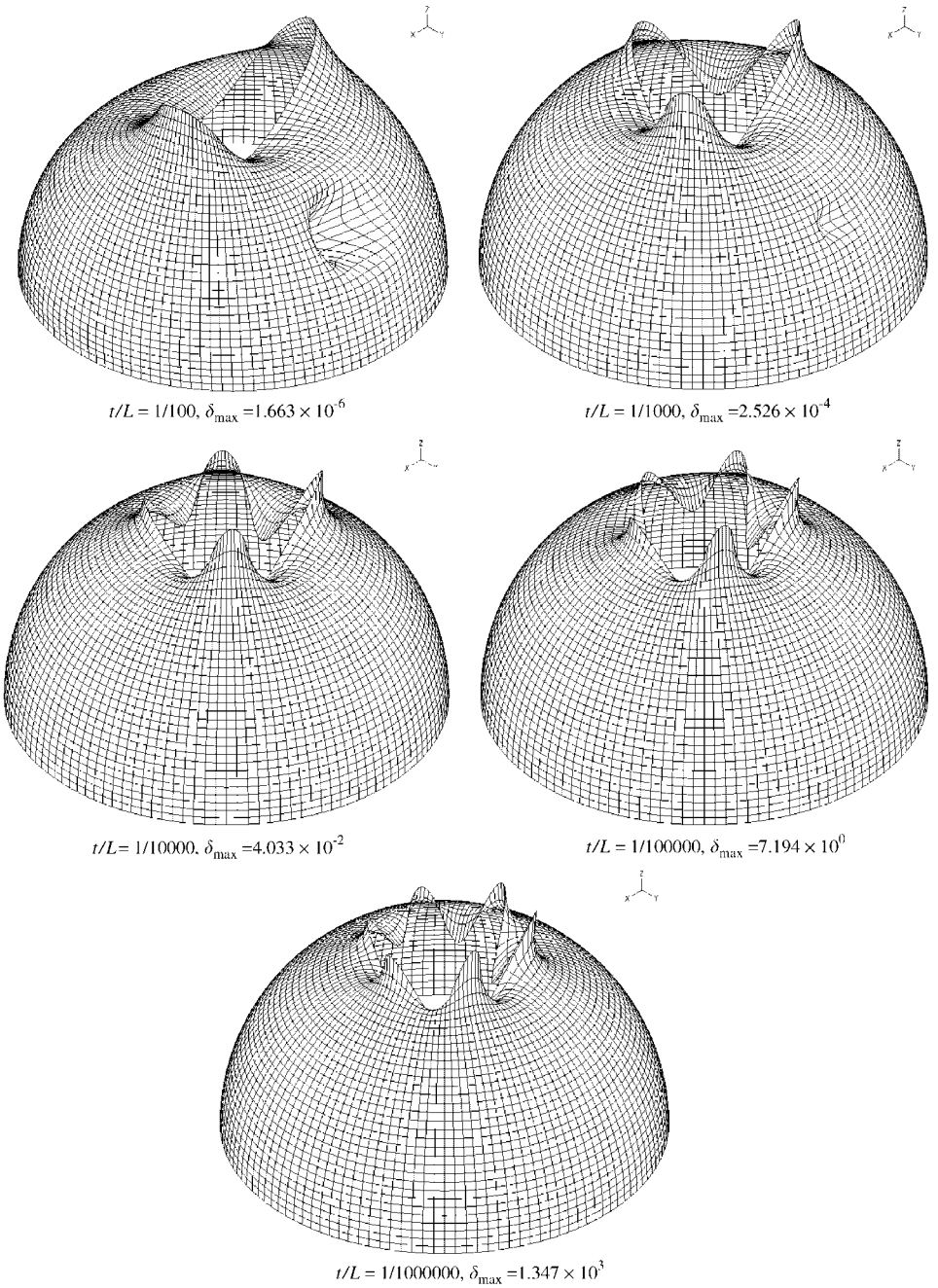

Figure 3. The deformed shapes as the shell thickness decreases, δ_{max} = the maximum outward total displacement for the constant applied loading.

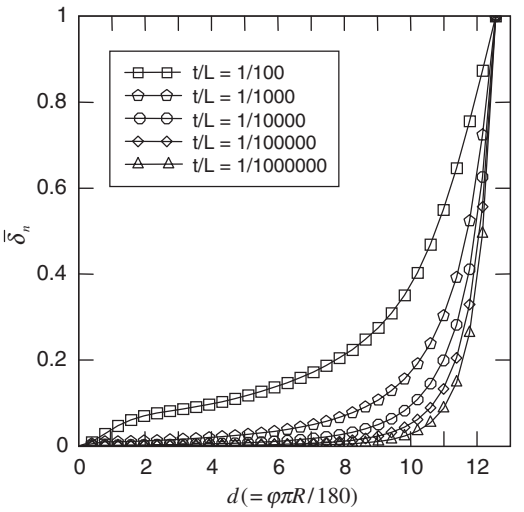

Figure 4. Displacement $\bar{\delta}_n$ in cross-sections in which maximum displacement occurs. The displacement is normalized to a unit value at the free edge.

Table II. Strain energy, load-scaling factor and proportion of bending energy as ε decreases.

$\varepsilon = t/L$	Strain energy	$R(\varepsilon)$	$\bar{\rho}$	$\tilde{R}(\varepsilon) = (\bar{\rho} - 1)/2$
1/100	1.08237E−06	0.290161	1.58021	0.290107
1/1000	2.50620E−05	0.129142	1.25834	0.129171
1/10 000	4.72692E−04	0.238421	1.47708	0.238542
1/100 000	1.62492E−02	0.363211	1.72666	0.363329
1/1 000 000	7.91755E−01	0.405001	1.81032	0.405158

increases as the shell thickness decreases. We would like to emphasize that this behaviour is seen in the linear static analysis of the shell and is not a consequence of buckling or large displacements. This behaviour is in accordance with the theoretical predictions published by Pitkäranta and Sanchez-Palencia [11].

Table II and Figure 5 give the total energy for each thickness of the shell and the calculated value of the scaling factor $\bar{\rho}$ using Equation (7) as the thickness decreases. In the calculation of $\bar{\rho}$, we used the specific thickness value considered and a change of 0.1% thereof. The table also gives the ratio of bending energy to total strain energy denoted as $R(\varepsilon)$ and calculated directly from the numerically obtained values of bending and total strain energies. In addition, the proportion of bending energy to total strain energy, denoted as $\tilde{R}(\varepsilon)$ calculated from the formula of Reference [6] using the load-scaling factor is given. We see that for this shell problem we do not seem to have convergence of the load-scaling factor, and of course neither for the value of R. This non-convergence of the load-scaling factor is associated with the increasing number of displacement oscillations at the free edge as the shell thickness decreases. We also note that the formula of Reference [6] gives for this problem surprisingly accurate results.

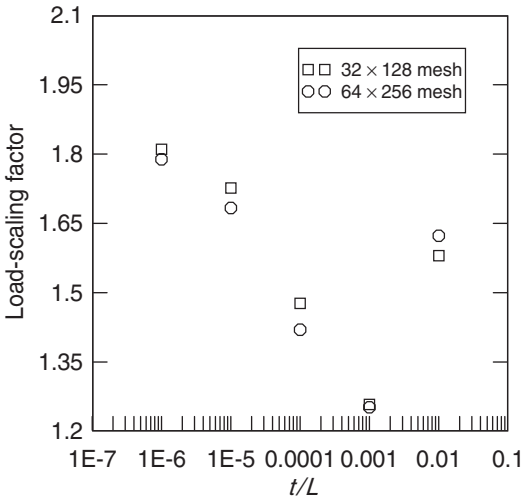

Figure 5. Load-scaling factor. The results when using the mesh of 32×128 elements and using the mesh of 64×256 elements.

Table III. Displacement components at the point right above the centre of the loading on the free boundary, point A, as ε decreases ($u_X = 0$ due to symmetry).

$\varepsilon = t/L$	u_Y	u_Z
1/100	−1.27E−06	−1.65E−06
1/1000	−1.37E−04	−2.66E−04
1/10 000	−1.87E−02	−4.16E−02
1/100 000	−2.96E+00	−7.13E+00
1/1 000 000	−5.11E+02	−1.29E+03

Finally, Figure 5 also shows the results obtained using a finer mesh of 64×256 elements, which was employed to see whether the results change substantially if the mesh is refined. A reasonable difference in the results is seen, since the finer mesh now represents the geometry, loading and the boundary layers more accurately. Table III gives the displacements at point A on the free edge of the shell, see Figure 1.

Figure 5 shows that the load-scaling factor for this shell problem first decreases and then increases. In order to obtain a scaling factor that actually fluctuates, we simply need to apply additional loading, since this is a linear problem. Figure 6 shows the shell with the original load plus an additional similarly applied distributed pressure load placed at the opposite side of the shell. Figure 7 gives the load-scaling factor calculated using Equation (7) for this shell problem. We note that the load-scaling factor and hence also the energies now oscillate, as the thickness of the shell decreases. Additional oscillations might be obtained by applying additional similar loadings offset at angles around the circumference.

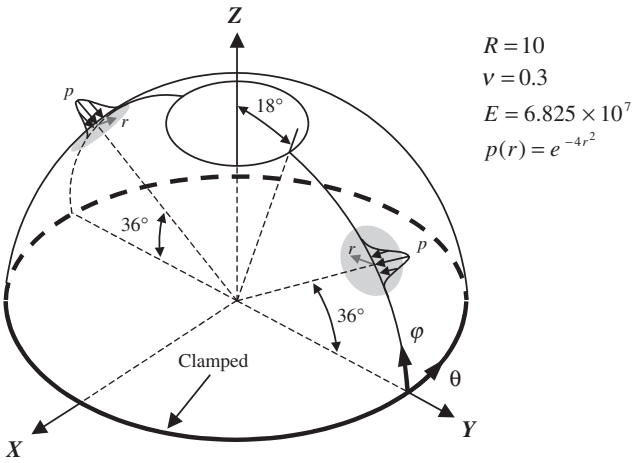

Figure 6. The shell problem with two load applications.

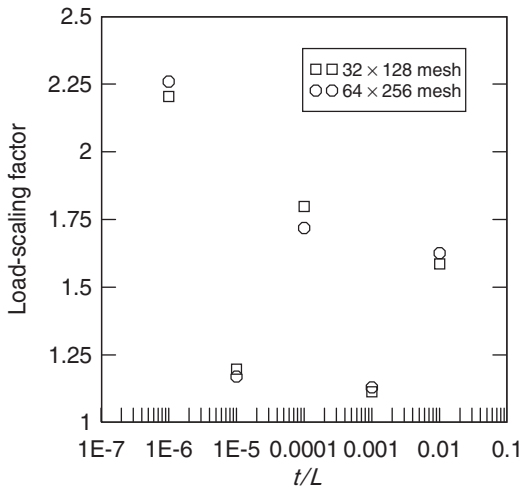

Figure 7. Load-scaling factor. The results when using the mesh of 32×128 elements and using the mesh of 64×256 elements.

Figure 7 shows also the results using the finer mesh of 64×256 elements. These results are merely given to show that the refinement of the mesh resulted again in reasonable differences. All further results given below correspond to the mesh of 32×128 elements.

Figures 8–10 show the calculated energy distributions as the shell thickness decreases. The results correspond to the total strain energy, bending strain energy only and membrane strain energy only, each time given as energies per unit surface area normalized by the total strain energy stored in the shell structure. These figures also show that we do not have a

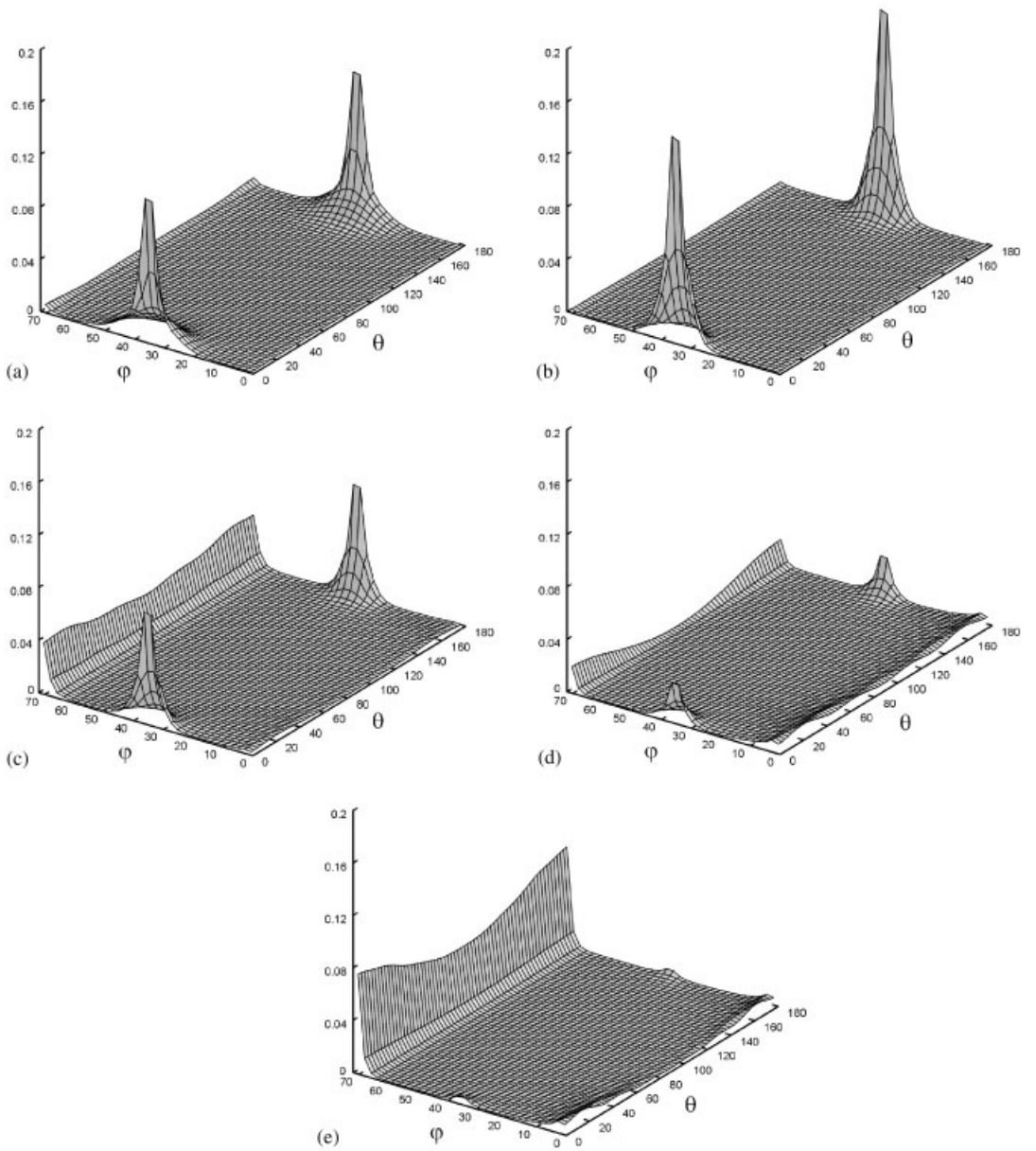

Figure 8. Strain energy distribution: (a) $\varepsilon = 0.01$; (b) $\varepsilon = 0.001$; (c) $\varepsilon = 0.0001$; (d) $\varepsilon = 0.00001$; and (e) $\varepsilon = 0.000001$.

membrane- or bending-dominated shell problem, and they show that the dominant displacements are bending dominated and occur in the boundary layer as the thickness decreases.

The displacement and stress response is clearly complex and highly dependent on the shell thickness. The results given underline the importance of using, for general shell analysis, only

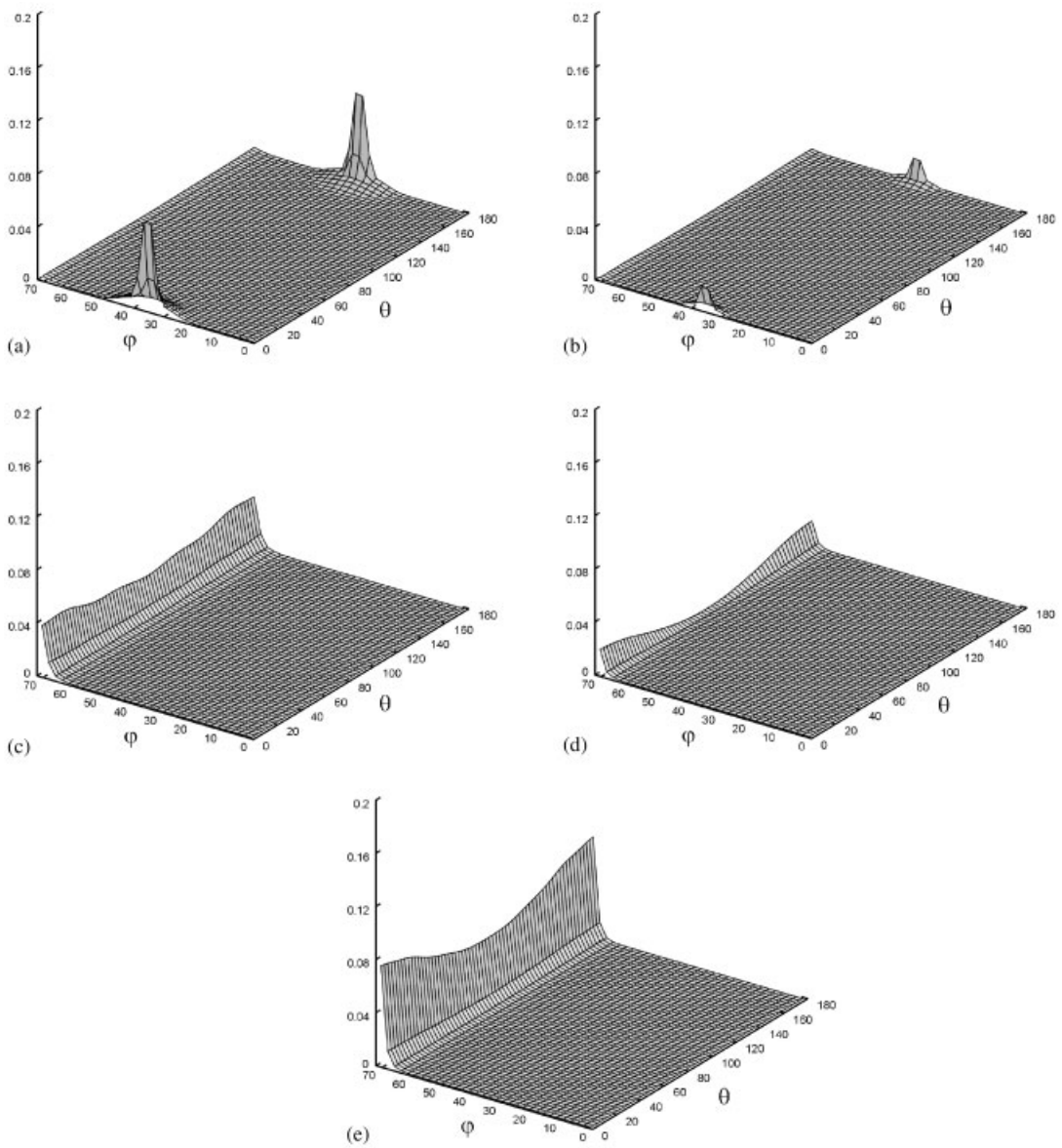

Figure 9. Bending energy distribution: (a) $\varepsilon = 0.01$; (b) $\varepsilon = 0.001$; (c) $\varepsilon = 0.0001$; (d) $\varepsilon = 0.00001$; and (e) $\varepsilon = 0.000001$.

finite element procedures that are able to solve accurately for membrane, bending and mixed states of stresses and energies.

We referred earlier to the original and modified Scordelis–Lo roof shell problems. The loading of the modified Scordelis–Lo roof problem is an element of V_m' whereas the loading

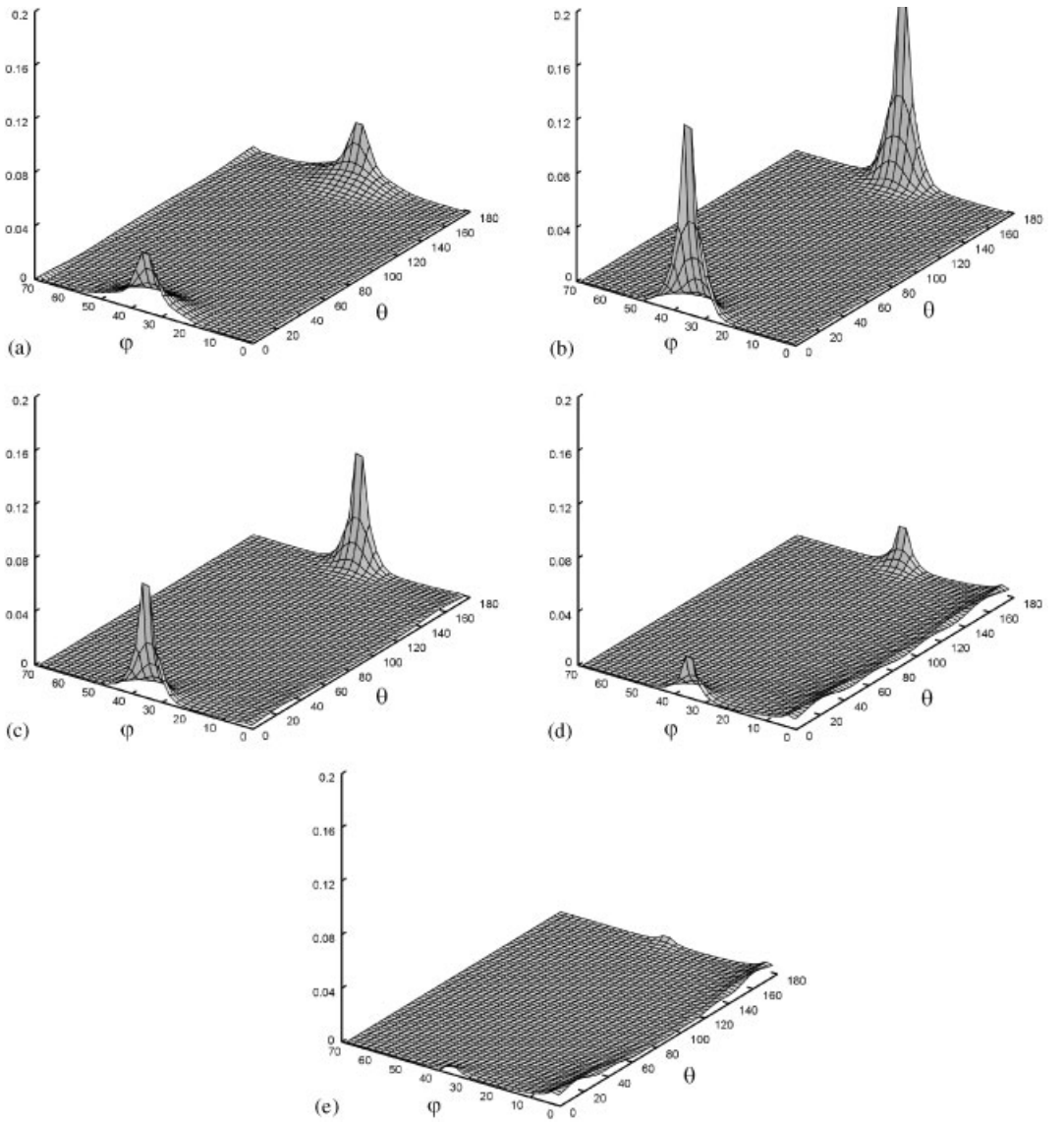

Figure 10. Membrane energy distribution: (a) $\varepsilon = 0.01$; (b) $\varepsilon = 0.001$; (c) $\varepsilon = 0.0001$; (d) $\varepsilon = 0.00001$; and (e) $\varepsilon = 0.000001$.

of the original Scordelis–Lo roof problem is not an element of V'_{m}. Therefore, the load-scaling factors are $\rho = 1$ and 1.75, respectively. Of course, the loading in the problem considered here is also not an element in V'_{m}, but the distinguishing feature is that in this problem V_{m} is not even a space of distributions. Hence, while the loading applied is (infinitely) smooth, it still is not an element of V'_{m}, and, physically, the possible displacements in V_{m} are very irregular which results in the unduly sensitive behaviour of the shell as its thickness is decreased.

Of course, as also further discussed in References [1, 2, 8–10, 14], this behaviour could be changed by a change in geometry or boundary conditions, including adding a stiffener at the free edge of the shell (which depending on the purpose of the shell may be required in practice).

3. CONCLUDING REMARKS

The common experience is that a shell problem can be identified to belong to one of the distinct categories of shell behaviours; namely bending-dominated, membrane-dominated, and mixed behaviours. Considering an asymptotic analysis for decreasing shell thickness, as pursued in recent years, the shell behaviour is usually associated with a well-defined load-scaling factor. This factor distinctly displays to which category the shell behaviour belongs and gives the ratios of energies (membrane and bending) asymptotically stored in the shell. The objective of this paper is to present a shell problem that does not have a well-defined load-scaling factor and for which the displacement and stress distributions do not uniformly converge to a limit state. Associated with this phenomenon, the ratios of membrane and bending energies to total strain energy also do not converge as the thickness of the shell decreases.

The non-convergence of the load-scaling factor is occurring with displacement oscillations in the boundary layer varying with the shell thickness. The fact that these changes in the oscillations are possible, and do occur, shows the high sensitivity of the shell problem.

While the problem is a very interesting one to solve numerically, it is, however, not a good test problem, on its own, for finite element methods. To test a finite element procedure, more insight is gained by solving (reasonably complex) pure membrane problems—to identify whether any consistency errors in the discretization scheme are under control—and to solve (reasonably complex) bending-dominated problems—to identify whether 'locking' is present [10, 15, 16]. Of course, once a finite element scheme has been shown to be effective for these problems, the method can also be confidently used for highly sensitive problems, such as the one discussed in this paper, in which then mixed stress states need be accurately computed. Indeed, then the shell problem discussed here is a valuable problem to solve in testing a finite element scheme.

The change in displacement and energy distributions observed in the analysis of the shell considered, as the thickness of the shell decreases, is a very interesting physical phenomenon and might well be exploited in practical applications of the future. Of course, other shell structural problems exhibit this kind of behaviour as well, and this whole class of shell problems, touched upon in this paper, deserves much further investigation. It would also be interesting to perform some physical (laboratory) experiments on the shell considered here and include non-linear effects in the theoretical and practical studies.

REFERENCES

1. Flügge W. *Stresses in Shells* (2nd edn). Springer: Berlin, 1973.
2. Farshad M. *Design and Analysis of Shell Structures.* Kluwer Academic Publishers: Dordrecht, 1992.
3. Pitkäranta J, Leino Y, Ovaskainen O, Piila J. Shell deformation states and the finite element method: a benchmark study of cylindrical shells. *Computer Methods in Applied Mechanics and Engineering* 1995; **128**:81–121.
4. Sanchez-Hubert J, Sanchez-Palencia E. *Coques Élastiques Minces—Propriétés Asymptotiques.* Masson: Paris, 1997.

5. Sanchez-Palencia E. General properties of thin shell solutions, propagation of singularities and their numerical incidence. In *Computational Fluid and Solid Mechanics*, Bathe KJ (ed.). Elsevier: Amsterdam, 2001; 454–455.
6. Baiocchi C, Lovadina C. A shell classification by interpolation. *Mathematical Models and Methods in Applied Sciences* 2002; **12**(10):1359–1380.
7. Auricchio F, Beirão da Veiga L, Lovadina C. Remarks on the asymptotic behaviour of Koiter shells. *Computers and Structures* 2002; **80**:735–745.
8. Chapelle D, Bathe KJ. *The Finite Element Analysis of Shells—Fundamentals.* Springer: Berlin, 2003.
9. Lee PS, Bathe KJ. On the asymptotic behaviour of shell structures and the evaluation in finite element solutions. *Computers and Structures* 2002; **80**:235–255.
10. Chapelle D, Bathe KJ. Fundamental considerations for the finite element analysis of shell structures. *Computers and Structures* 1998; **66**:19–36, 711–712.
11. Pitkäranta J, Sanchez-Palencia E. On the asymptotic behaviour of sensitive shells with small thickness. *Comptes Rendus de l' Academie des Sciences Paris*, *Série II* 1997; **325**:127–134.
12. Bathe KJ. *Finite Element Procedures.* Prentice-Hall: Englewood Cliffs, NJ, 1996.
13. Chapelle D, Bathe KJ. The mathematical shell model underlying general shell elements. *International Journal for Numerical Methods in Engineering* 2000; **48**:289–313.
14. Steele CR. Asymptotic analysis and computation for shells. In *Analytical and Computational Models of Shells*, CED-vol. 3, Noor AK, Belytschko T, Simo JC (eds). ASME: New York, 1989.
15. Bathe KJ, Iosilevich A, Chapelle D. An evaluation of the MITC shell elements. *Computers and Structures* 2000; **75**:1–30.
16. Bathe KJ. The inf–sup condition and its numerical evaluation for mixed finite element methods. *Computers and Structures* 2001; **79**:243–252, 971.

